Δελτίο της Ελληνικής Γεωλογικής Εταιρίας, τομ. XLVII , 2013
Πρακτικά 13ου Διεθνούς Συνεδρίου, Χανιά, Σεπτ. 2013

Bulletin of the Geological Society of Greece, vol. XLVII 2013
Proceedings of the 13th International Congress, Chania, Sept. 2013

MINERALOGY AND CHEMISTRY OF AMPHIBOLES AND THERMOBAROMETRY OF PAPIKION MT PLUTON, RHODOPE, NORTHERN GREECE

Drakoulis A.[1], Koroneos A.[1], Soldatos T.[1] and Papadopoulou L.[1]

[1]Aristotle University of Thessaloniki, Faculty of Science, School of Geology, Dept of Mineralogy-Petrology-Economic Geology.

Abstract

Papikion Mt pluton which intrudes Kardamos Dome, consists of biotite (Bi), hornblende (Hbl) and biotite-hornblende (Bi-Hbl) bearing rock types. In this work the relationship among the amphiboles of each Hbl-bearing rock type is studied. Moreover, their minimum crystallization pressure and temperature are estimated. The amphiboles of the Hbl granodiorite (GRD), the Bi-Hbl diorite (DR) and the Hbl diorite (DR) are classified mainly as magnesiohornblende and ferrohornblende and the amphiboles of the Bi-Hbl GRD as ferroedenite and hanstingsite. It is to note that some samples contain amphibole crystals showing a sieved texture with quartz. These sieved amphiboles have no chemical differences from the rest amphibole crystals. This texture can probably derive from the breakdown of mafic minerals of an assimilated xenolith such as pyroxenes and hornblende itself, leaving quartz. Using the Al-in-hornblende geobarometer and the plagioclase-hornblende geothermometer), minimum crystallization pressures from 4.6 to 5.2 kbar and temperatures from 700 to 740 °C were estimated for the Bi-Hbl GRD. The DR shows crystallization pressures ranging from 6.4 to 7.4 kbar and temperatures ranging from 620 to 700 °C. The Hbl GRD shows the lowest P-T values, thus an average crystallization pressure about 3 kbar and an average temperature about 600 °C were estimated.
Key words: *sieved hornblende, crystallization pressure and temperature, subsolidus cooling.*

Περίληψη

Ο πλουτωνίτης του Παπικίου Όρους που διεισδύει στο Δόμο του Κάρδαμου, αποτελείται από Bi, Hbl και Bi-Hbl τύπους πετρωμάτων. Σε αυτή την εργασία μελετάται η σχέση μεταξύ των αμφιβόλων του κάθε πετρογραφικού τύπου που τις περιέχει. Οι αμφίβολοι του κεροστιλβικού γρανοδιορίτη (Hbl GRD), του βιοτιτικού-κεροστιλβικού διορίτη (Bi-Hbl DR)και του κεροστιλβικού διορίτη (Hbl DR) ταξινομούνται κυρίως ως μαγνησιοκεροστίλβες και σιδηροκεροστίλβες και οι αμφίβολοι του βιοτιτικού-κεροστιλβικού γρανοδιορίτη (Bi-Hbl GRD) ως σιδηροεδενίτες και χαστινγκσίτες. Πρέπει να σημειωθεί ότι ορισμένα δείγματα περιέχουν κρυστάλλους αμφιβόλου που παρουσιάζουν κοσκινινοειδή υφή με χαλαζία. Αυτές οι κοσκινοειδείς αμφίβολοι δεν διαφέρουν χημικά από τις υπόλοιπες. Η υφή αυτή μπορεί να προέρχεται από την αποδόμηση των φεμικών ορυκτών ενός αφομοιωμένου ξενόλιθου όπως οι πυρόξενοι αλλά και η ίδια η κεροστίλβη, αφήνοντας πίσω χαλαζία. Χρησιμοποιώντας το γεωβαρόμετρο Al στην κεροστίλβη και το γεωθερμόμετρο κεροστίλβης-πλαγιοκλάστου, υπολογί-

στηκαν ελάχιστη πίεση κρυστάλλωσης 4,6 - 5,2 kbar και θερμοκρασίες 700 - 740 °C για το Bi-Hbl DR και 6,4 έως 7,4 kbar και θερμοκρασίες από 620 έως 700 °C στην ομάδα DR.. Ο Hbl GRD δείχνει τις χαμηλότερες τιμές P-T, με μέση πίεση κρυστάλλωσης περίπου 3 kbar και με μέση θερμοκρασία περίπου 600 °C.
Λέξεις κλειδιά: *Κοσκινοειδής κεροστίλβη, πίεση και θερμοκρασία κρυστάλλωσης, ψύξη σε συνθήκες υπο-αγχιτηκτικής κατάστασης.*

1. Introduction

In the eastern Rhodope two large tectonic windows appear, called Kesebir-Kardamos Dome and Biela Reka–Kechros Dome. The greek part of Kesebir-Kardamos Dome is known as Kardamos Complex. The Papikion Mt. Pluton, intruding Kardamos Dome, consists of biotite (Bi), hornblende (Hbl) and biotite-hornblende (Bi-Hbl) bearing rock types. A noteworthy observation concerns the morphology of some Hbl crystals in some samples. In detail, these crystals are sieved, mainly subhedral in shape and enclose randomly anhedral quartz. This work aims at studying the mineralogy and chemistry of the amphiboles of Hbl-bearing rock types and contributes to the estimation of the crystallization conditions. Efforts are made in order to explain the origin of the above mentioned sieved hornblendes.

2. Geological Setting

The evolution of the Rhodope massif has been extensively studied through the past years. The Greek Rhodope massif has been divided into two tectonic units: the Lower Tectonic Unit (LTU), also known as Pangaion and the Upper Tectonic Unit (UTU) also known as Sidironero (Papanikolaou and Panagopoulos, 1981, Mposkos, 1989, Mposkos and Liati, 1993). The LTU extends towards the NW, into Bulgaria, where it is called Pirin Unit. This terrain represents a microcontinent with a carbonate platform that cores the large antiform from the Rila Mountains to the Thassos island through the Pirin and Pangaion mountains (e.g. Kronberg et al., 1970, Kronberg and Raith, 1977). The LTU is mainly composed of a succession of orthogneiss and migmatitic gneiss with a few paragneiss occurrences in Bulgaria (Ivanov, 1988) and a succession of alternating pelitic gneisses, amphibolites and marbles in Greece (Mposkos, 1998, Krohe and Mposkos, 2002). The UTU is of higher metamorphic grade (upper amphibolite-facies and, at least partly, granulite-facies) and is separated from the LTU (upper greenschist-facies to lower amphibolite-facies) by a major WNW trending thrust plane, known as the Nestos Thrust Zone (Papanikolaou and Panagopoulos, 1981, Zachos and Dimadis, 1983, Mposkos, 1989, Gerdjikov and Milev, 2005). The UTU comprises interlayered amphibolites, marbles, metapelitic schists and various gneisses enclosing eclogite and metaophiolite lenses (Ivanov, 1988, Burg et al., 1996).

According to Burg (2012) LTU is exposed also in eastern Rhodope as a string of four separated domes. These are, from northwest to southeast, the Chepinska, Arda, Kesebir and Biela Reka "units" in Bulgaria; the last two are called Kardamos (Mposkos and Krohe, 2000) and Kechros (Mposkos and Krohe, 2000) in Greece. These domes expose monotonous, quartz-feldspathic, strongly deformed gneisses of dioritic composition intruded by metagranitoids, some of which are presumably syntectonic. The Kesebir (Bulgaria)-Kardamos (Greece) is a subelliptical extensional gneiss dome that trends NE–SW (Bonev et al., 2006, Krenn et al., 2010) (Fig. 1a).

The Papikion Mt. pluton intrudes Kardamos Dome (Fig. 1a&b). It spreads from Iasmos in the east, to Komotini to the west and from the Xanthi-Komotini fault in the south to the Greek-Bulgarian borders to the north. This pluton, with characteristic gneissic texture, covers about 100 km^2 in the SW part of Kardamos Dome in Greece. It is bordered by marbles to the SW, where typical skarn minerals appear, epidote and garnet, and by gneiss to the NE, intruding the Kardamos Dome (Bonev et al., 2006 and references therein). The thickness of the skarn zone ranges from 0.5 m to 1.5 m. The gneisses represent the lower unit of Kardamos Dome and the marbles represent the

intermediate unit, therefore the Papikion Mt. pluton intrudes both the lower and intermediate units of the Kardamos Dome.

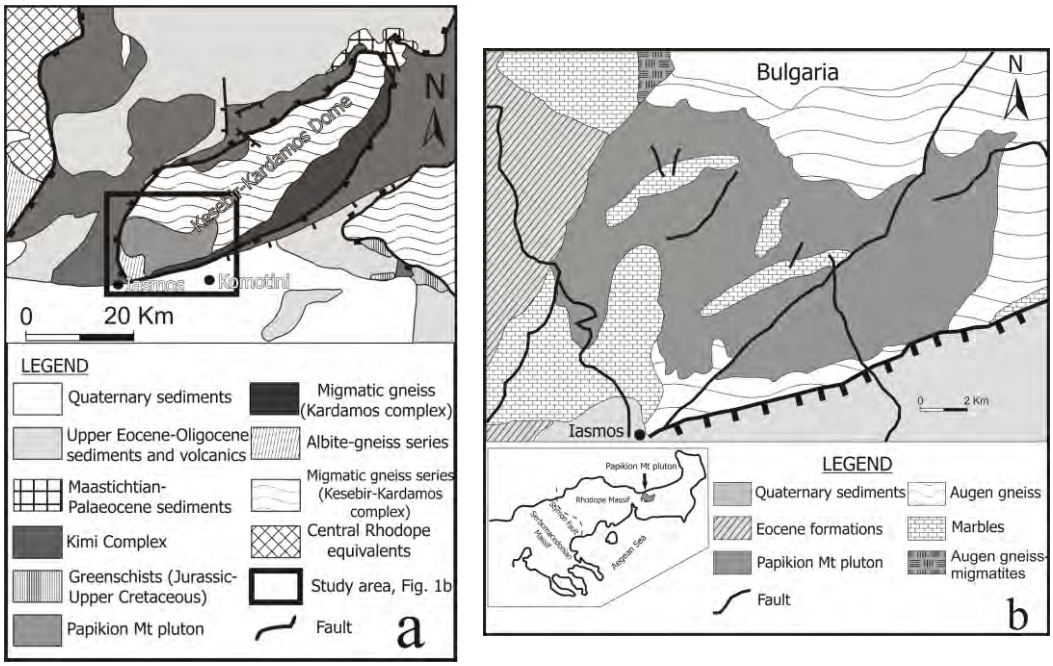

Figure 1 – a) Geological map of Kesebir-Kardamos Dome (Modified after Bonev et al., 2006). b) Geological map of Papikion Mt pluton (Modified after Dimades and Zachos, 1985).

3. Petrology

Papikion Mt pluton consists mainly of six rock types which have been classified on the basis of field observations, mineralogical composition and the Q'-ANOR diagram (Streckeisen & Le Maitre, 1979, not shown). These types are biotite granite (Bi GR), biotite granodiorite (Bi GRD), biotite hornblende granodiorite (Bi-Hbl GRD), hornblende granodiorite (Hbl GRD), biotite hornblende diorite (Bi-Hbl DR) and hornblende diorite (Hbl DR). Aplitic dykes intrude the above rock types. The Bi GRD contains fine to medium grained, ellipsoidal, mafic microgranular enclaves (MME) with length ranging from 5 to 30 cm. Xenoliths, mainly of amphibolitic composition, also exist mostly in Bi & Bi-Hbl GRD. About 200 samples were collected from the plutonic and the basement rocks and a group of 65 samples have been analyzed by X-Ray Fluorescence (XRF) for major and trace elements (as part of the PhD thesis of the first author). In general, all the rocks are evidently foliated. The relationship among the rock types is rather obscure. There is no field evidence of one rock type intruding the other. In addition, there are some locations where mingling phenomena are characteristic.

In all Hbl-bearing rocks, the hornblende is the main mafic mineral. The Hbl DR contains in average 60% Hbl, the Bi-Hbl DR contains 42% Hbl, while the Hbl GRD contains 30% Hbl and Bi-Hbl GRD contains 18% Hbl.

4. Petrography and Mineral Chemistry

In general, hornblende has colours ranging from light green to brown and shows no zoning. In some cases, it is enclosed by biotite although elsewhere biotite encloses hornblende. Many samples, mostly those collected at the margins of the pluton, have gneissic texture, however, hornblende crystals do not display any preferred orientation. Hbl forms euhedral to subhedral

(from now on will be called “normal”) crystals and in some samples sieved crystals (Fig. 2 a&b). Sieved crystals are mainly subhedral in shape and enclose randomly anhedral quartz. However, samples with both Hbl textures, normal and sieved, were observed.

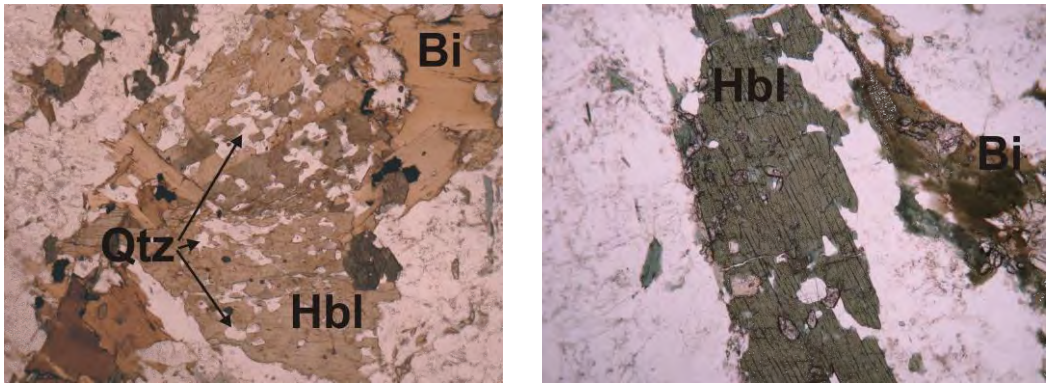

Figure 2 - Photos of hornblende a) with a quartz sieved texture and b) with normal texture. The long dimension of each photo corresponds to 4mm, parallel Nicols.

Representative samples of the Hbl-bearing rock types were selected for microanalyses. Mineral chemical analyses were carried out at the Scanning Microscope Laboratory, A.U.Th., using a JEOL JSM-840A Scanning Electron Microscope (SEM) equipped with an Energy Dispersive Spectrometer (EDS) with 20kV accelerating voltage and 0.4 mA probe current. Pure Co was used as an optimization element. For SEM observations, the samples were coated with carbon – average thickness of 200 Å – using a vacuum evaporator JEOL-4X.

The results of representative amphibole analyses from each Hbl-bearing rock type are given in Table 1. Ferric iron was estimated according to Schumacher (1997). The Si content varies between from 6.29 to 7.47 atoms per formula unit (apfu). According to the classification diagram of Leake (1997), all the amphiboles belong to the calcic group. Amphiboles of the Bi-Hbl GRD plot in the area of ferroedenite and hastingsite (Fig. 3a). On the other hand, the amphiboles of Bi-Hbl DR and Hbl DR, plot mainly in the magnesiohornblende field and the ferrohornblende field (Fig. 3b). Finally, the amphiboles of Hbl GRD are displayed only in the magnesiohornblende field (Fig. 3c). From Figures 3b and 3c, it is obvious that sieved hornblendes are not chemically different from the normal ones. Plagioclases appear to be homogeneous and no zoning was observed. Plagioclase compositions range from An_{23} to An_{40} in all Hbl-bearing rock types.

5. Thermobarometry

The average, minimum and maximum crystallization pressures for each rock type as resulted from the application of amphibole barometry are given in Fig. 6a. In all cases chemical analyses were chosen from the rim of the amphibole crystals and constraints of each barometer were taken into account.

The higher mean pressure values were found in the group of DR, while the lower in Hbl GRD. The highest crystallization pressure was found in the DR with the Schmidt geobarometer (6.9 ±0.6 kbar). To calculate the pressure by the geobarometer of Anderson and Smith (1995) a mean temperature of 740 °C was accepted for Bi-Hbl GRD, 700 °C for the DR group and 600 °C for Hbl GRD. Mean temperatures were estimated by the amphibole-plagioclase geothermometer (Holland and Blundy, 1994).

The application of the amphibole-plagioclase geothermometer gave values, in average, from 600 (± 40)°C (Hbl GRD) to 725 (± 40)°C (Bi Hbl GRD) (Fig. 6b). Plagioclase compositions were in the range of An_{25}-An_{35}.

6. Discussion

Amphiboles are present both with sieved texture enclosing randomly anhedral quartz and with normal texture. No chemical difference was observed among the two.

According to Collins (2003) and Collins and Collins (2002 and references therein) sieved hornblende texture has been ascribed to K- and Si-metasomatism after solidification of the plutonic rock. In this case, an initial mafic igneous rock, uniform in composition and fabric, crystallized from magma. If this rock is deformed so that fluids can enter and cause metasomatism at temperatures below melting conditions, a granite with a uniform appearance can be the final product. During this process, plagioclase in the original mafic rock could be partially replaced by K-feldspar while the rest recrystallizes as sodic plagioclase. Si-metasomatism causes replacement of hornblende and/or biotite by quartz resulting in sieve texture. This could explain the occurrence of a low-temperature mineral, such as quartz, enclosed in the high-temperature hornblende crystals. Because most of the ferromagnesian silicates are replaced by quartz, the final product is a granite whose composition lies on or near the eutectic minimum. In magmatic or metasomatic granites, the mineral assemblages are the same and stable at the same P-T conditions.

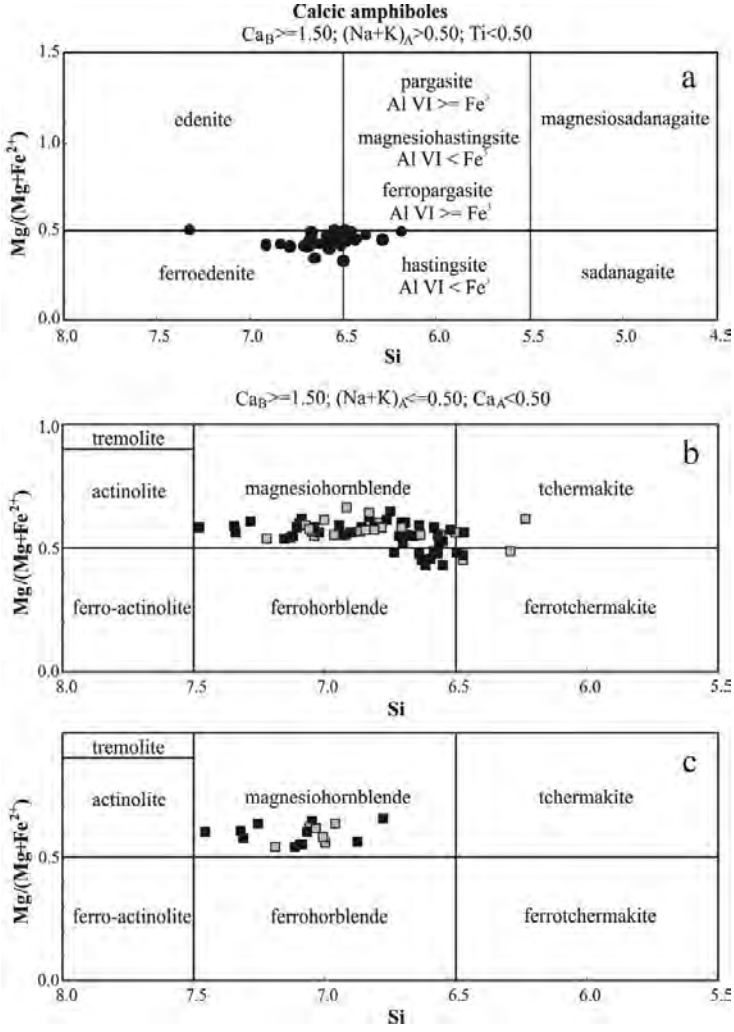

Figure 3 - Classification diagrams after Leake et al. (1997, 2003) a) Bi Hbl GRD, b) Bi-Hbl DR and Hbl DR, c) Hbl GRD; grey squares: sieved crystals, black squares: normal crystals.

According to Beard et al. (2005) sieved hornblende may be the result of bulk assimilation of xenoliths from the magma during crust-mantle mixing. In this case, xenoliths containing mica or amphibole are incorporated into host magma and are subjected to dehydration melting producing plagioclase, pyroxene, Fe-Ti oxides, and hydrous melt. Due to partial melting, the xenolith begins to disintegrate and "xenolithic melt" and crystals are mixed into the host magma. At this stage, pyroxenes and oxides undergo hydration crystallization reactions that lead to the formation of feldspars, amphiboles and micas. Replacement of pyroxene by amphibole results in the formation of quartz at amphibole-pyroxene contact. Eventually, when pyroxene is consumed, a quartz-sieved hornblende texture remains.

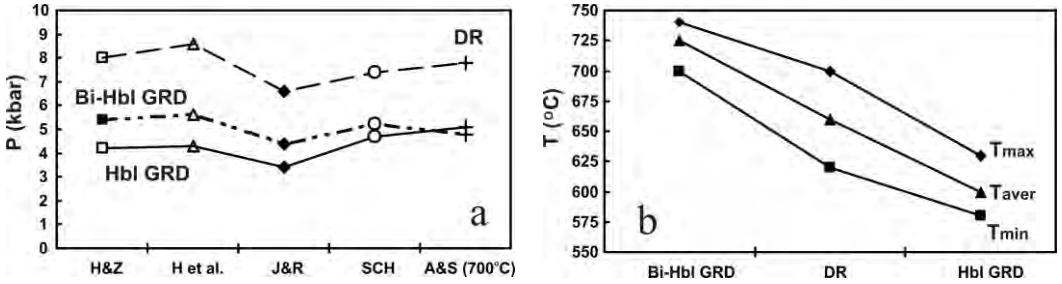

Figure 6 a & b – a) Maximum, minimum and average values of crystallization pressures of Hbl-bearing rock types of Papikion Mt pluton, based on amphibole barometry. H&Z: Hammarstrom and Zen (1986), H et al.: Hollister et al. (1987), J&R: Johnson & Rutherford (1989), SCH: Schmidt (1992) and A&S: Anderson and Smith (1995).b) Maximum, minimum and average values of crystallization temperatures of Hbl-bearing rock types of Papikion Mt pluton, based on the amphibole-plagioclase geothermometer.

There are many geothermometers used in metamorphic rocks and many of them are applied to plutonic rocks. The specificity of plutonic rocks is that mineral phases can crystallize in a wide range of pressures and temperatures and it is uncertain whether they have reached equilibrium conditions during magma crystallization. Many minerals continue to equilibrate and change composition after magma crystallization, during cooling in the solid state (subsolidus cooling), indicating continuous reaction with the melt. Ion exchange between minerals can continue well below the solidus temperature. The use of many different thermometers can lead to reliable conclusions concerning the conditions of magma crystallization. The amphibole-plagioclase geothermometer of Holland and Blundy (1994) used in the Hbl-bearing rocks of Papikion Mt. yields average temperatures, with an error of ± 40 °C, of 600 °C (Hbl GRD), 660 °C (DR) and 725 °C (Bi Hbl GRD) that are considered low for dioritic and granodioritic magmas. These temperatures possibly represent the equilibrium temperatures of amphibole and plagioclase, i.e. the time that ion diffusion ceased rather than crystallization temperatures.

7. Conclusions

The hornblende occurs as the basic mafic component in Bi-Hbl GRD and Bi-Hbl DR and is the only mafic mineral of Hbl GRD and Hbl DR. According to the nomenclature diagrams, the amphiboles of the Hb GRD, the Bi-Hbl DR and the Hbl DR are classified mainly as magnesiohornblende and ferrohornblende and the amphiboles of the Bi-Hbl GRD are ferroedenite and hanstingsite. The sieved crystals of hornblende differ from the normal ones only morphologically and not chemically. This texture can probably derive from the destruction of mafic minerals such as pyroxenes and hornblende itself, leaving quartz. Some samples present particular gneiss texture, but the crystals of hornblende in these samples are not oriented. The low temperatures estimated for the Papikion Mt pluton could be ascribed to high oxygen fugacity partial pressure (fO2), as been noted for other granitoids, particularly for I-type granitic rocks

Table 1 - Representative analyses of amphiboles from each Hbl-bearing rock type of Papikion Mt pluton based on 23 O.

Sample	15			925			602			603			911			14			220		
	core	int	Rim	core	int	rim	core	int	rim	core	int	rim	core	int	rim	core	int	rim	core	rim	rim
SiO_2	44.91	45.06	45.87	47.28	46.39	46.36	43.94	45.94	42.27	44.97	42.92	43.49	48.34	51.21	47.85	44.09	43.25	43.37	42.62	41.30	41.52
TiO_2	0.42	0.50	0.54	0.77	0.65	0.53	0.54	0.39	0.50	0.39	0.79	0.66	0.44	0.00	0.22	0.60	0.51	0.48	0.64	0.84	0.77
Al_2O_3	11.02	11.88	11.70	10.90	12.16	11.23	12.30	8.68	15.01	10.66	11.83	12.71	7.29	4.91	7.82	9.50	9.71	9.68	10.26	8.09	9.95
FeO	17.21	15.26	16.46	14.43	14.65	14.19	17.84	16.78	17.30	18.40	18.46	18.87	15.25	15.95	15.81	20.44	20.66	20.71	20.36	26.20	20.83
MnO	0.20	0.57	0.36	0.39	0.41	0.49	0.54	0.60	0.68	0.67	0.47	0.52	0.58	0.56	0.53	0.73	0.92	0.58	0.34	0.40	0.46
MgO	9.95	10.48	10.06	10.16	10.37	10.60	9.59	11.35	8.20	8.83	8.43	7.56	12.01	12.26	12.05	8.50	8.69	8.14	8.62	6.09	8.68
CaO	12.56	12.44	12.02	11.74	11.40	11.98	11.33	12.55	11.96	12.13	12.31	12.10	12.49	12.48	12.71	11.63	12.20	12.16	12.12	11.65	12.12
Na_2O	0.89	0.66	1.01	0.69	0.87	1.14	1.01	0.82	1.54	0.88	0.76	0.95	1.05	0.54	0.83	1.36	1.05	1.38	1.29	0.98	1.36
K_2O	0.43	0.36	0.34	0.52	0.54	0.53	0.58	0.67	0.43	0.74	0.89	0.69	0.82	0.48	0.60	1.45	1.59	1.54	1.75	1.88	1.67
Total	97.73	97.31	98.37	96.89	97.49	97.05	97.65	97.78	97.89	97.67	97.03	97.57	98.28	98.37	98.42	98.30	98.58	98.06	98.02	97.43	97.37
Si	6.664	6.642	6.716	6.965	6.781	6.845	6.501	6.795	6.294	6.737	6.498	6.550	7.110	7.479	7.001	6.682	6.537	6.628	6.496	6.501	6.383
Al IV	1.336	1.358	1.284	1.035	1.219	1.155	1.499	1.205	1.706	1.263	1.502	1.450	0.890	0.521	0.999	1.318	1.463	1.372	1.504	1.499	1.617
T	*8.000*	*8.000*	*8.000*	*8.000*	*8.000*	*8.000*	*8.000*	*8.000*	*8.000*	*8.000*	*8.000*	*8.000*	*8.000*	*8.000*	*8.000*	*8.000*	*8.000*	*8.000*	*8.000*	*8.000*	*8.000*
Al VI	0.592	0.705	0.737	0.857	0.876	0.799	0.646	0.308	0.927	0.619	0.610	0.807	0.374	0.323	0.350	0.379	0.267	0.372	0.339	0.002	0.187
Ti	0.047	0.055	0.060	0.085	0.072	0.059	0.060	0.044	0.056	0.044	0.090	0.074	0.049	0.000	0.024	0.068	0.058	0.055	0.073	0.099	0.089
Fe^{3+}	0.314	0.324	0.198	0.004	0.181	0.014	0.553	0.459	0.240	0.215	0.321	0.135	0.018	0.033	0.261	0.241	0.492	0.191	0.318	0.628	0.521
Cr	0.000	0.000	0.000	0.000	0.000	0.000	0.000	0.000	0.000	0.000	0.000	0.000	0.000	0.000	0.000	0.000	0.000	0.000	0.000	0.000	0.000
Mg	2.202	2.303	2.197	2.231	2.260	2.332	2.115	2.503	1.821	1.972	1.903	1.697	2.634	2.670	2.630	1.920	1.957	1.855	1.959	1.429	1.988
Fe^{2+}	1.822	1.558	1.810	1.774	1.610	1.739	1.626	1.617	1.914	2.090	2.017	2.243	1.858	1.915	1.673	2.350	2.119	2.456	2.276	2.821	2.157
Mn	0.023	0.055	0.000	0.048	0.002	0.057	0.000	0.070	0.042	0.060	0.059	0.044	0.067	0.059	0.062	0.042	0.106	0.071	0.035	0.021	0.058
C	*5.000*	*5.000*	*5.000*	*5.000*	*5.000*	*5.000*	*5.000*	*5.000*	*5.000*	*5.000*	*5.000*	*5.000*	*5.000*	*5.000*	*5.000*	*5.000*	*5.000*	*5.000*	*5.000*	*5.000*	*5.000*
Mg	0.000	0.000	0.000	0.000	0.000	0.000	0.000	0.000	0.000	0.000	0.000	0.000	0.000	0.000	0.000	0.000	0.000	0.000	0.000	0.000	0.000
Fe^{2+}	0.000	0.000	0.008	0.000	0.000	0.000	0.028	0.000	0.000	0.000	0.000	0.000	0.000	0.000	0.000	0.000	0.000	0.000	0.000	0.000	0.000
Mn	0.002	0.016	0.045	0.001	0.049	0.004	0.067	0.005	0.043	0.025	0.002	0.022	0.005	0.009	0.004	0.052	0.011	0.004	0.010	0.032	0.001
Ca	1.996	1.965	1.886	1.853	1.786	1.895	1.796	1.989	1.908	1.947	1.996	1.952	1.969	1.953	1.992	1.889	1.976	1.991	1.979	1.965	1.997
Na	0.002	0.019	0.061	0.147	0.166	0.101	0.109	0.006	0.049	0.029	0.002	0.026	0.026	0.038	0.004	0.059	0.013	0.005	0.011	0.003	0.002
B	*2.000*	*2.000*	*2.000*	*2.000*	*2.000*	*2.000*	*2.000*	*2.000*	*2.000*	*2.000*	*2.000*	*2.000*	*2.000*	*2.000*	*2.000*	*2.000*	*2.000*	*2.000*	*2.000*	*2.000*	*2.000*
Na	0.255	0.170	0.227	0.052	0.082	0.224	0.180	0.230	0.395	0.227	0.220	0.251	0.274	0.114	0.231	0.339	0.294	0.402	0.371	0.297	0.405
K	0.082	0.068	0.064	0.097	0.102	0.101	0.109	0.126	0.082	0.142	0.172	0.133	0.153	0.089	0.112	0.281	0.306	0.301	0.341	0.377	0.328
A	*0.337*	*0.238*	*0.291*	*0.149*	*0.184*	*0.325*	*0.288*	*0.356*	*0.477*	*0.370*	*0.392*	*0.385*	*0.427*	*0.202*	*0.344*	*0.620*	*0.600*	*0.703*	*0.712*	*0.674*	*0.733*

Table 1 (continue) - Representative analyses of amphiboles from each Hbl-bearing rock type of Papikion Mt pluton based on 23 O.

Sample	15			925			602			603			911			14			220		
	core	int	Rim	core	int	rim	core	int	rim	core	int	rim	core	int	rim	core	int	rim	core	rim	rim
SiO_2	44.91	45.06	45.87	47.28	46.39	46.36	43.94	45.94	42.27	44.97	42.92	43.49	48.34	51.21	47.85	44.09	43.25	43.37	42.62	41.30	41.52
TiO_2	0.42	0.50	0.54	0.77	0.65	0.53	0.54	0.39	0.50	0.39	0.79	0.66	0.44	0.00	0.22	0.60	0.51	0.48	0.64	0.84	0.77
Al_2O_3	11.02	11.88	11.70	10.90	12.16	11.23	12.30	8.68	15.01	10.66	11.83	12.71	7.29	4.91	7.82	9.50	9.71	9.68	10.26	8.09	9.95
FeO	17.21	15.26	16.46	14.43	14.65	14.19	17.84	16.78	17.30	18.40	18.46	18.87	15.25	15.95	15.81	20.44	20.66	20.71	20.36	26.20	20.83
MnO	0.20	0.57	0.36	0.39	0.41	0.49	0.54	0.60	0.68	0.67	0.47	0.52	0.58	0.56	0.53	0.73	0.92	0.58	0.34	0.40	0.46
MgO	9.95	10.48	10.06	10.16	10.37	10.60	9.59	11.35	8.20	8.83	8.43	7.56	12.01	12.26	12.05	8.50	8.69	8.14	8.62	6.09	8.68
CaO	12.56	12.44	12.02	11.74	11.40	11.98	11.33	12.55	11.96	12.13	12.31	12.10	12.49	12.48	12.71	11.63	12.20	12.16	12.12	11.65	12.12
Na_2O	0.89	0.66	1.01	0.69	0.87	1.14	1.01	0.82	1.54	0.88	0.76	0.95	1.05	0.54	0.83	1.36	1.05	1.38	1.29	0.98	1.36
K_2O	0.43	0.36	0.34	0.52	0.54	0.53	0.58	0.67	0.43	0.74	0.89	0.69	0.82	0.48	0.60	1.45	1.59	1.54	1.75	1.88	1.67
Total	97.73	97.31	98.37	96.89	97.49	97.05	97.65	97.78	97.89	97.67	97.03	97.57	98.28	98.37	98.42	98.30	98.58	98.06	98.02	97.43	97.37
Si	6.664	6.642	6.716	6.965	6.781	6.845	6.501	6.795	6.294	6.737	6.498	6.550	7.110	7.479	7.001	6.682	6.537	6.628	6.496	6.501	6.383
Al IV	1.336	1.358	1.284	1.035	1.219	1.155	1.499	1.205	1.706	1.263	1.502	1.450	0.890	0.521	0.999	1.318	1.463	1.372	1.504	1.499	1.617
T	*8.000*	*8.000*	*8.000*	*8.000*	*8.000*	*8.000*	*8.000*	*8.000*	*8.000*	*8.000*	*8.000*	*8.000*	*8.000*	*8.000*	*8.000*	*8.000*	*8.000*	*8.000*	*8.000*	*8.000*	*8.000*
Al VI	0.592	0.705	0.737	0.857	0.876	0.799	0.646	0.308	0.927	0.619	0.610	0.807	0.374	0.323	0.350	0.379	0.267	0.372	0.339	0.002	0.187
Ti	0.047	0.055	0.060	0.085	0.072	0.059	0.060	0.044	0.056	0.044	0.090	0.074	0.049	0.000	0.024	0.068	0.058	0.055	0.073	0.099	0.089
Fe^{3+}	0.314	0.324	0.198	0.004	0.181	0.014	0.553	0.459	0.240	0.215	0.321	0.135	0.018	0.033	0.261	0.241	0.492	0.191	0.318	0.628	0.521
Cr	0.000	0.000	0.000	0.000	0.000	0.000	0.000	0.000	0.000	0.000	0.000	0.000	0.000	0.000	0.000	0.000	0.000	0.000	0.000	0.000	0.000
Mg	2.202	2.303	2.197	2.231	2.260	2.332	2.115	2.503	1.821	1.972	1.903	1.697	2.634	2.670	2.630	1.920	1.957	1.855	1.959	1.429	1.988
Fe^{2+}	1.822	1.558	1.810	1.774	1.610	1.739	1.626	1.617	1.914	2.090	2.017	2.243	1.858	1.915	1.673	2.350	2.119	2.456	2.276	2.821	2.157
Mn	0.023	0.055	0.000	0.048	0.002	0.057	0.000	0.070	0.042	0.060	0.059	0.044	0.067	0.059	0.062	0.042	0.106	0.071	0.035	0.021	0.058
C	*5.000*	*5.000*	*5.000*	*5.000*	*5.000*	*5.000*	*5.000*	*5.000*	*5.000*	*5.000*	*5.000*	*5.000*	*5.000*	*5.000*	*5.000*	*5.000*	*5.000*	*5.000*	*5.000*	*5.000*	*5.000*
Mg	0.000	0.000	0.000	0.000	0.000	0.000	0.000	0.000	0.000	0.000	0.000	0.000	0.000	0.000	0.000	0.000	0.000	0.000	0.000	0.000	0.000
Fe^{2+}	0.000	0.000	0.008	0.000	0.000	0.000	0.028	0.000	0.000	0.000	0.000	0.000	0.000	0.000	0.000	0.000	0.000	0.000	0.000	0.000	0.000
Mn	0.002	0.016	0.045	0.001	0.049	0.004	0.067	0.005	0.043	0.025	0.002	0.022	0.005	0.009	0.004	0.052	0.011	0.004	0.010	0.032	0.001
Ca	1.996	1.965	1.886	1.853	1.786	1.895	1.796	1.989	1.908	1.947	1.996	1.952	1.969	1.953	1.992	1.889	1.976	1.991	1.979	1.965	1.997
Na	0.002	0.019	0.061	0.147	0.166	0.101	0.109	0.006	0.049	0.029	0.002	0.026	0.026	0.038	0.004	0.059	0.013	0.005	0.011	0.003	0.002
B	*2.000*	*2.000*	*2.000*	*2.000*	*2.000*	*2.000*	*2.000*	*2.000*	*2.000*	*2.000*	*2.000*	*2.000*	*2.000*	*2.000*	*2.000*	*2.000*	*2.000*	*2.000*	*2.000*	*2.000*	*2.000*
Na	0.255	0.170	0.227	0.052	0.082	0.224	0.180	0.230	0.395	0.227	0.220	0.251	0.274	0.114	0.231	0.339	0.294	0.402	0.371	0.297	0.405
K	0.082	0.068	0.064	0.097	0.102	0.101	0.109	0.126	0.082	0.142	0.172	0.133	0.153	0.089	0.112	0.281	0.306	0.301	0.341	0.377	0.328
A	*0.337*	*0.238*	*0.291*	*0.149*	*0.184*	*0.325*	*0.288*	*0.356*	*0.477*	*0.370*	*0.392*	*0.385*	*0.427*	*0.202*	*0.344*	*0.620*	*0.600*	*0.703*	*0.712*	*0.674*	*0.733*

(Soltani and Carr, 2007, Toummite et al., 2012). Conclusion about the conditions of the crystallization of Papikion Mt pluton is that the pluton penetrated in deep and in relatively high pressures, about 5 kbar, considering the thin skarn zone (0,5-1,5 m approx.) of the pluton with the marbles (Bucher and Frey, 2002). Also the use of amphibole-plagioclase thermometer shows that the system has prevailed ion diffusion in the solid state to succeed a balance.

8. Acknowledgments

The first author wants to thank SCF (State Scholarship Foundation) for the financial support in the early years of his graduate studies.

9. References

Anderson J.L. and Smith D.R. 1995. The effect of temperature and oxygen fugacity on Al-in-hornblende barometry, *Amer. Mineral.*, 80, 549-559.

Beard J.S., Ragland P.C. and Crawford M.L. 2005. Reactive bulkassimilation: A model for crust-mantle mixing insilicic magmas, *Geological Society of America*, 33(8), 681–684.

Bonev N., Burg J.-P. and Ivanov Z. 2006. Mesozoic-Tertiary structural evolution of an extensional gneiss dome–the Kesebir-Kardamos dome, eastern Rhodope (Bulgaria-Greece), *Int. J. Earth. Sci.*, 95(2), 318-340.

Bucher K. and Frey M. 2002. *Petrogenesis of metamorphic rocks*, 7th edition, Springer-Verlag Berlin, Heidelberg, Germany, 341pp.

Burg J-P, Ricou L-E, Ivanov Z, Godfriaux I, Dimov D and Klain L. 1996. Syn-metamorphic nappe complex in the Rhodope Massif. Structure and kinematics, *Terra Nova*, 8, 6–15.

Burg J.P. 2012. Rhodope: From Mesozoic convergence to Cenozoic extension. In: Emmanuel Skourtsos and Gordon S. Lister (eds), *The Geology of Greece. Review of petro-structural data in the geochronological frame Journal of the Virtual Explorer*, Electronic Edition, ISSN 1441-8142, volume 42, paper 1.

Collins L.G. 2003. Transition from magmatic to K-metasomatic processes in granodiorites and Pyramid Peak granite, Fallen Leaf Lake 15-Minute Quadrangle, California. ISSN 1526-5757, no. 48, available online at: http://www.csun.edu/~vcgeo005/Nr48Fallen.pdf

Collins L.G. and Collins J.B. 2002. Myrmekite formation at Temecula, California, revisited: A photomicrographic essay illustrating replacement textures. ISSN 1526-5757, no. 43, available online at: http://www.csun.edu/~vcgeo005/Nr43Temecula.pdf

Dimades E. and Zachos S. 1985.Geological map of Rhodope 1:200.000. *IGME*.

Gerdjikov I. and Milev P. 2005. Nestos Shear Zone and structure of the metamorphic basement in the area south of Mesta graben, SW Bulgaria, *C.R. Acad. bulg. Sci.*, 58(2), 197-204.

Hammarstrom J.M. and Zen E.-A. 1986. Aluminium in hornblende: an empirical igneous geo-barometer, *American Mineralogist*, 71, 1297-1313.

Holland T. and Blundy J. 1994. Non-ideal interactions in calcic amphiboles and their bearing on amphibole-plagioclase thermometry, *Contrib. Mineral. Petrol.*, 116, 433-447.

Hollister L.S., Grisom G.C., Peters E.K., Stowell H.H. and Sisson V.B. 1987. Confirmation of the empirical correletion of Al in hornblende with pressure of solidification of calc-alkaline plutons, *American Mineralogist*, 72, 231-239.

Ivanov Ž. 1988. Aperçu général sur l'évolution géologique et structurale du massif des Rhodopes dans le cadre des Balkanides, *Bull. Soc. géol. Fr.*, 8, 227-240.

Johnson M.C. and Rutherford M.J. 1989. Experimental calibration of the aluminium-in-hornblende geobarometer with application to Long Valley caldera (California) volcanic rocks, *Geology*, 17, 837-841.

Krenn K., Bauer C., Proyer A., Klötzli U. and Hoinkes G. 2010. Tectonometamorphic evolution of the Rhodope orogen, *Tectonics*, 29.

Krohe A. and Mposkos E. 2002. Multiple generations of extensional detachments in the Rhodope Mountains (northern Greece): evidence of episodic exhumation of high-pressure rocks, in:

Blundell D. J., Neubauer F. and Von Quadt A. (eds). *The timing and location of major ore deposits in an evolving orogen*. Geological Society, Special Publication 204, London, 151-178.

Kronberg B., Meyer W. and Pilger A. 1970. Geologie der Rila-Rhodope-Masse zwischen Strimon und Nestos (Nord-Griechenland), *Beih. geol. Jb.*, 88, 133-180.

Kronberg B. and Raith M. 1977. Tectonic and metamorhism of the Rhodope crystalline complex in the Eastern Greek Macedonia and parts of the Western Thrace, *N. Jb. Geol. Paleont. Mh.*, 11, 697-704.

Leake B.E., Wooley A.R., Arps C.E.S., Birch W.D., Gilbert M.C., Grice J.D., Hawthorne F.C., Kato A., Kisch H.J., Krivovichev V.G., Linthout K., Laird J., Mandarino J.A., Maresh W.V., Nickel E.H., Rock N.M.S., Schumacher J.C., Smith D.C., Stephenson N.C.N., Ungaretti L., Whittaker E.J.W. and Youzhi G. 1997. Nomenclature of Amphiboles: Report of the Subcommittee on Amphiboles of the International Mineralogical Association, Commission on New Minerals and Mineral Names, *Can. Mineral.*, 35, 219-246.

Mposkos E. 1989. High-pressure metamorphism in gneisses and schists in the East Rhodope zone (N. Greece), *Mineral. Petrol.*, 41, 25-39.

Mposkos E. 1998. Cretaceous and tertiary tectonometamorphic events in Rhodope zone (Greece). Petrological and geochronological evidences, *Bull Geol Soc Greece*, 32(3):59–67.

Mposkos E. and Liati A. 1993. Metamorphic evolution of metapelites in the high-pressure terrane of the Rhodope zone, Northern Greece, *Can. Mineral.*, 31(2), 401-424.

Mposkos E.and Krohe A. 2000. Petrological and structural evolution of continental high-pressure (HP) metamorphic rocks in the Alpine Rhodope domain. In: Panaydes, I., Xenophontos, C., Malpas, J. (eds), *Proceedings of the 3rd international conference geology East Mediterranean*. Geol Surv Nicosia, Cyprus 1, 221–232.

Papanikolaou D. and Panagopoulos A. 1981. On the structural style of the Southern Rhodope, Greece, *Geol. Balc.*, Sofia, 11 (3), 13-22.

Schmidt M.W. 1992. Amphibole composition in tonalite as a function of pressure: an experimental calibration of the Al-in-hornblende barometer, *Contrib. Mineral. Petrol.*, 110, 304-310.

Schumacher J.C. 1997. The estimation of the proportion of ferric iron in the electron-microprobe analysis of amphiboles, *Can. Mineral.* 35, 238-246.

Soltani A. and Carr P.F. 2007. Thermobarometry of Ca-amphibole in a Typical Low–temperature I-type Granite from Kashmar, Iran, *Journal of Technology & Education*, 1(3), 47-54.

Streckeisen A. and Le Maitre R.W. 1979. A chemical approximation to the modal QAPF classification of the igneous rocks, *N. Jb. Min. Abh*., 136, 169-206.

Toummite A., Ikenne M. and Beraaouz E.H. 2012. Geothermobarometry of Askaoun Pluton in Ouzellarh-Sirwa Promontory (Central Anti-Atlas; Morocco), *Open Journal of Geology*, 2, 136-147.

Zachos S. and Demades E. 1983. The geotectonic position of the Scaloti-Echinos granite and its relationship to the metamorphic formation of Greek Westarn and Central Rhodope, *Geol. Balc.*, 13(5), 17-24.